21st Century Asian air pollution impacts glacier in northwestern Tibet

M. Roxana Sierra-Hernández[1], Emilie Beaudon[1], Paolo Gabrielli[1,2], and Lonnie G. Thompson[1,2]

[1]Byrd Polar and Climate Research Center, The Ohio State University, Columbus, OH, 43210, USA
[2]School of Earth Sciences, The Ohio State University, Columbus, OH, 43210, USA

Correspondence to: M. Roxana Sierra-Hernández (sierra-hernandez.1@osu.edu)

Abstract. Over the last four decades, Asian countries have undergone significant economic development leading to rapid urbanization and industrialization. Consequently, fossil fuel consumption has risen dramatically worsening the air quality in Asia. Fossil fuel combustion emits particulate matter containing toxic metals that can adversely affect living organisms, including humans. Thus, it is imperative to investigate the temporal and spatial extent of metal pollution in Asia. Recently, we reported a continuous and high-resolution 1650–1991 ice core record from the Guliya ice cap in northwestern Tibet, China showing contamination of Cd, Pb and Zn during the 20th century. Here, we present a new continuous and high-resolution ice core record of trace metals from the Guliya ice cap that comprises the years between 1971 and 2015, extending the 1650–1991 ice core record into the 21st century. Non-crustal Cd, Pb, Zn and Ni enrichments increased since the 1990s relative to the 1971-1990 period reaching a maximum in 2008. The enrichments of Cd, Pb, Zn, and Ni increased by ~75 %, 35 %, 30 %, and 10 %, respectively during the 2000–2015 period relative to 1971–1990. The observed TE enrichments likely originated primarily from fossil fuel combustion and biomass burning with likely contributions from industrial processes, and agricultural activities from South Asia (Pakistan, Afghanistan, India, Nepal), Central Asia, and the Xinjiang province in western China. This new record demonstrates that the current emissions in Asia are impacting remote high-altitude glaciers in the region and that mitigation policies and technologies should be enforced to improve the air quality as economic development continues in most Asian countries.

1 Introduction

Atmospheric trace elements (TE), including toxic metals (e.g., Hg, Pb, Cd) have dramatically increased since the 19th century due to human activities (Pacyna and Pacyna, 2001; Tian et al., 2015). Some TEs are highly toxic and harmful to an array of animals, plants and humans. Atmospheric TEs can originate from natural sources/processes in the environment such as windborne dust, wildfires, sea-spray aerosols, volcanic activity, and from vegetation (Nriagu, 1989a, b). TEs are also released into the atmosphere by human activities such as: 1) the combustion of fossil fuels including coal, oil and its distillates (e.g., gasoline, jet fuel, diesel), 2) biomass burning (e.g., wood, dung, agricultural waste); 3) industrial processes such as mineral extraction, and metal production;4) agriculture practices that include the use of fertilizers and pesticides; and 5) waste disposal (Pacyna and Pacyna, 2001; Christian et al., 2010; Zhang et

al., 2014; Chen et al., 2015; Singh et al., 2018). These activities, especially high temperature processes, emit fine (< 2.5 μm) particulate matter ($PM_{2.5}$) containing toxic metals such as As, Cd, Pb, and Zn (Richaud et al., 2004; Xu et al., 2004; Reddy et al., 2005; Alves et al., 2010; Christian et al., 2010) that due to its small size, can reside in the atmosphere for over a week, thereby allowing it to be transported and deposited far from its initial sources (e.g., onto remote glaciers) (Pacyna and Pacyna, 2001; Marx and McGowan, 2010).

Since the 1970s, Asian countries such as China, India, Pakistan, Nepal, Bangladesh and others have undergone significant and rapid economic growth, leading to considerable urbanization and industrialization in the region. Consequently, fossil fuel consumption has risen dramatically in most of these countries worsening the air quality. In particular, China and India, the second and fifth largest economies in the world according to the International Monetary Fund, are respectively the largest and third largest emitters of both CO_2 and $PM_{2.5}$ (Crippa et al., 2018; EDGARv4.3.2, 2017).

In 1999, the Chinese government implemented the "Western Development" policy in the 10th five-year plan to improve the quality of the environment in the east and to transfer energy (West to East energy program) and mineral resources from the west to the rest of the country (Lai, 2002; Chen et al., 2010; Dong and Yang, 2014). For this purpose, the necessary infrastructure (e.g., airports, railways, highways, water infrastructure, power lines) was built. As a result, energy consumption (Jianxin, 2016) and atmospheric emissions (Liu et al., 2015) have been increasing significantly in western China.

In particular, the Xinjiang Uygur Autonomous Region, situated in an arid region of northwestern China, has become important for the Western Development implementation because of its location on the new Silk Road, a project to modernize and build new infrastructure to connect China with the West, and its large reserves of oil, gas, and coal (Chen et al., 2010; Dong and Yang, 2014; Fridley et al., 2017). Three mountain ranges shape the topography of this province: the Altai on the northern border, Tien Shan in the center, and the western Kunlun Mountains, where the Guliya ice cap is located (see below), along the southern border with Tibet (Fig. 1a).

Pakistan, to the southeast of Xinjiang, gained its independence in 1947 after which its population rose very rapidly becoming the world's sixth most populated country by 2003 (UN, 2017). Although Pakistan's economic growth has been much lower than that of China and India, urban Pakistani cities are among the most polluted in the world (WHO, 2016) due to the high population growth, industrialization and a significant increase in motor vehicles that lack emission controls and use low quality gasoline/diesel.

For the year 1995, Pacyna and Pacyna (2001) estimated that non-ferrous metal production was the largest source of As, Cd, Cu, In, and Zn, coal combustion was a major source of Cr, Hg, Mn, Sb, Se, Sn, and Tl, and oil combustion was a major source of Ni and V, both worldwide and in Asia. For the same year, these authors estimated that leaded gasoline was the primary source of Pb worldwide as well as in Asia. However, changes in emissions of atmospheric TEs have occurred during the 21st century in Asia due to the following: 1) China and India emerged as the fastest growing economies and most populated countries in the world (UN, 2017); 2) developing countries such as Pakistan, Nepal and Bangladesh have significantly increased their national economic activities since the 1980s–1990s; 3)

temporal and regional variations in the implementation of control emission technologies and air quality standards (often higher concentrations than those recommended by the World Health Organization); 4) leaded gasoline was banned in 2000 in China, India, and Nepal and in 2002 in Pakistan, while it is still consumed in Afghanistan. Therefore, it is imperative to study the spatial and temporal effects of these new pollution sources and their resulting impacts on the environment.

Atmospheric emission estimates are associated with large uncertainties due to inaccurate statistical information, the lack of field data, and limited temporal and spatial coverage of observations. Thus, natural registers of past environmental conditions such as glaciers, which are influenced only by deposition of atmospheric species, are essential for reconstructing time series of atmospheric metal depositions (Hansson et al., 2015; Cooke and Bindler, 2015; Gabrielli and Vallelonga, 2015; Marx et al., 2016) that can be further used by modelers to reconstruct past emissions and project future atmospheric contamination trends.

Recently, we obtained a 350-year (1650–1991) high-resolution TE record (Sierra-Hernández et al., 2018) using an ice core drilled in 1992 from the Guliya ice cap located in northwestern China, specifically in Tibet's Kunlun Mountains (35° 17.37' N; 81° 29.73' E; 6200 m a.s.l.) (Thompson et al., 1995) (Fig. 1a). Outside of the Arctic and Antarctica, the glaciers in the Kunlun Mountains, along with those in Tibet and the Himalayas, are the largest reservoir of ice on the globe and are commonly referred to as the "Third Pole". This glacial region is the source for numerous rivers in Asia which provide water to hundreds of millions of people. The 1992 Guliya TE record showed that long-distance emissions from coal combustion in Europe were likely deposited on the ice cap between 1850 and 1940 (Sierra-Hernández et al., 2018). Additionally, Pb, Cd, and Sn enrichments were detected between 1975 and 1991. The origin of these more recent enrichments could not be determined as more anthropogenic sources have emerged, especially in this region.

Here, we use a new ice core retrieved from Guliya in 2015 to extend the 1650–1991 TE records into the 21st century (1971–2015) and to determine the impacts of the recent emission changes in Asia on the western Kunlun Mountains glaciers. New emission inventories of air pollutants, in particular the Emissions Database for Global Atmospheric Research (EDGAR v4.3.2) which compiles a comprehensive dataset of air pollutants between 1970 and 2012, are used here to attribute possible sources. This study fills a temporal and spatial gap in the investigation of atmospheric toxic trace metals in Northwestern China where atmospheric emission data are limited.

2 Methodology

2.1 Guliya cores

In 2015, two ice cores (309.73 m and 72.40 m long) were extracted from the plateau of the Guliya ice cap (6200 m a.s.l), in close proximity to the 1992 drilling site. The timescale was constructed by annual layer counting using three fixed horizons at 2015 (surface of the glacier), at 1992 corresponding to the surface of the 1992 core (at 6 m in the shallow core), and at 1963 (at 10.9 m in the shallow core determined by beta radioactivity from the Arctic thermonuclear tests). Annual layers were determined using both cores by matching the signals of at least three different

parameters (Cl^- and Na^+, dust and Ca^{2+}, SO_4^{2-}, and $\delta^{18}O$). Dating uncertainties are estimated at 1–2 years between the fixed points and may be the result of the very low annual accumulation (~230 mm water equivalent) and surface-alteration processes such as snow redistribution through wind. Details of the drilling operation, the ice cores, and the timescale can be found in Thompson et al. (2018).

2.2 Sample preparation and ICP-SFMS analysis

The preparation of the samples and their analysis were performed following the same procedures adopted for the 1992 Guliya core samples (Sierra-Hernández et al., 2018). Briefly, 159 ice samples comprising the years 1971 (11 m) to 2015 (0.06 m) were cut from the 309.73 m long-deep ice core. To ensure the analysis of 3–4 samples $year^{-1}$, the sample resolution was adjusted between 4.5 and 11 cm accordingly. The samples were rinsed three times with nanopure water (18.3 MΩ) in a class-100 cleanroom and placed in acid pre-cleaned LDPE containers (Nalgene) to melt. Once melted, samples were transferred into acid pre-cleaned LDPE vials where nitric acid (HNO_3, Optima for Ultra Trace Element Analysis, Fisher Scientific) was added to obtain a 2 % (v/v) acidified sample. The samples were then stored in the cleanroom for a 30-day period during which the acid leaching process took place. At the end of the 30-day period, the samples were immediately analyzed or stored at –32 °C.

Twenty-nine TEs (Ag, Al, As, Ba, Bi, Cd, Co, Cr, Cs, Cu, Fe, Ga, Li, Mg, Mn, Mo, Na, Nb, Ni, Pb, Rb, Sb, Sn, Sr, Ti, Tl, U, V, and Zn) were measured in the samples by Inductively Coupled Plasma Sector Field Mass Spectrometry (ICP-SFMS) (Element 2) (Sierra-Hernández et al., 2018; Beaudon et al., 2017). Trace elements were quantified using linear calibration curves constructed from external standards analyzed before and after the samples.

Detection limits, procedural blanks, and accuracy results are presented in Table S1. Detection limits correspond to three standard deviations of the concentration of 10 blank measurements (2 % optima HNO_3 aqueous solution) and fluctuate between 0.01 pg g^{-1} for Bi to 0.2 ng g^{-1} for Fe and 0.4 ng g^{-1} for Na (Beaudon et al., 2017; Sierra-Hernández et al., 2018). To verify that the sampling and decontamination procedures did not add TEs to the ice core samples, procedural blanks were made with nanopure water and analyzed with the ice core samples (Uglietti et al., 2014). Their TE concentrations are considered negligible for all TEs, apart from Nb (9 %), as they were lower than 2 % of the corresponding median concentration. The accuracy of the ICP-SFMS was determined each day of analysis using a 20-fold dilution of a TMRain-95 certified solution (Environment Canada). The obtained TE concentrations fell within the uncertainty limits in the certificate of analysis.

2.3 Non-crustal contribution

Enrichment Factors (EF) and Excess concentrations are used to assess the crustal and non-crustal (e.g., anthropogenic) origins of each TE.

The EF is obtained following Eq. (1)

$$EF = [TE\ /\ Fe]_{ice} / [TE\ /\ Fe]_{PSA} \quad (1)$$

where $[TE\ /\ Fe]_{ice}$ corresponds to the ratio of a particular TE concentration to that of Fe in an ice sample and $[TE\ /\ Fe]_{PSA}$ is the respective ratio in dust samples used as potential source area (PSA). Eight dust samples were collected during the 1992 and 2015 Guliya field expeditions and are used here as PSAs. For details about the collection sites, the preparation and analysis of the PSA samples, and EFs derived from PSAs, the reader is referred to Sierra-Hernández (2018). Briefly, approximately 0.1-0.5 g of PSA sample was added to an acid pre-cleaned LDPE container with ultrapure water. The solution was mixed by agitation and settled ~2 minutes. For the ICP-SFMS analysis, 10 ml of supernatant was used and prepared like the ice samples.

Similar to the previous Guliya TEs study, Fe was chosen as the crustal reference due to its stability and high abundance in soil and rocks (Wedepohl, 1995), its high concentration both in the ice core samples and the PSAs, and the ability of the ICP-SFMS to measure Fe with high accuracy and precision (Uglietti et al., 2014). Additionally, Fe is highly correlated with Al (r = 1) and with Ba (r = 0.98). EFs calculated using Al and Ba as crustal references showed no significant differences to EFs relative to Fe which indicates that the choice of Fe as a crustal TE to calculate EFs did not affect the results (Sierra-Hernández et al., 2018).

The EFs relative to the PSA are particularly small since the composition of the PSA is a much closer representation of the crustal background of the ice samples compared to those obtained using the upper continental background (Wedepohl, 1995). Therefore, Excess concentration is also used here as in our previous publication (Sierra-Hernández et al., 2018) to further corroborate the EF increases observed.

Excess concentrations are calculated following Eq. (2)

$$Excess = [TE]_{ice} - \left([TE/Fe]_{pre-industrial} \times [Fe]_{ice}\right) \quad (2)$$

$[TE]_{ice}$ and $[Fe]_{ice}$ are the concentrations of a particular TE and of Fe in the sample; $[TE/Fe]_{pre-industrial}$ is the median of the TE concentration to the Fe concentration ratio during the pre-industrial period (1650-1750). The pre-industrial period corresponds the oldest part of the 1992 Guliya record (Sierra-Hernández et al., 2018) between 1650 and 1750, ~30 years before the Industrial Revolution began in Europe. The Excess concentration provides the TE concentration difference between TE deposition after and before the pre-industrial period.

To be consistent with our previous Guliya TEs publication, a TE will be considered of non-crustal origin (enriched) when increases in EF and Excess concentration are significantly different from its background (pre-industrial levels), using both a two-sample t-test for averages and the Mann–Whitney test for medians ($p < 0.01$).

2.4 Statistical analysis

All statistical analyses, including factor analysis, cluster analysis, Mann–Whitney tests for medians, two-sample t-tests for averages, and Mann–Kendall trend tests, were performed using Minitab 17 and 18. The Mann–Whitney test and the two-sample t-test were applied to the entire data set and subdivided into three groups: 1971–1990, 1990–2000, and 2000–2015.

3 Results and discussion

The time series of Cd, Pb, Zn, Ni, and Al concentrations, Excess concentrations and EFs are presented as 5-year running means in Fig. 2. The concentrations show high variability between 1971 and 1990 that decreases after 1990 perhaps as a result of the decreasing frequency of dust storms in the region (Thompson et al., 2018).

The Excess concentrations and EFs of Cd, Ni, Pb, and Zn increase after ~1990 and continue to increase more rapidly and significantly after 2000. Their EF averages increase by ~10 % for all four TEs during 1990–2000, and during 2000–2015 by 75 % (Cd), 35 % (Pb), 30 % (Zn), and 10 % (Ni) relative to the 1971–1990 period.

A comparison between the 1992 and the 2015 Guliya TE records is discussed in the Supplement (Fig. S1-S2). The 1992 Guliya TE records show that enrichments of Pb and Cd begin ~1975 while the 2015 Guliya record shows they continue to rise into the 21st century until ~2008 when the Cd enrichment started to decrease. In addition to these TEs, the 2015 record exhibits clear increases in Zn and Ni EFs since the 1990s into the 21st century, and similar to Cd, they decrease after 2008. The Zn enrichment began to increase after 1975 similar to Pb and Cd; however, the signal may have been overwhelmed by its crustal component in the 1992 core record rendering it undetectable.

A factor analysis method was performed to assess the shared variability among TEs to determine possible common sources (Sierra-Hernández et al., 2018). Most of the variance (94%) is explained by both Factor 1 (73 %) and Factor 2 (21 %) (Table S2). Similar to the 1992 TE results, TEs of crustal origin (e.g., Al, As, Ba, Fe, Mg, Mn, Ti, and V) fall into Factor 1. In Fig. S3 the time series of Factor 1 scores are compared with the ice core concentrations of dust particles ($\rho = 0.20$, $p = 0.2$) and with the typical crustal TEs, Fe and Al. Water-soluble TEs (e.g., Na, Sr), which are deposited in the form of salts (evaporites) or carbonates, contribute to Factor 2 (Sierra-Hernández et al., 2018) (Table S2). This is shown in the Factor 2 time series (Fig. S4) which has significant ($p < 0.001$) correlations with the ions Cl^- ($\rho = 0.83$), NO_3^- ($\rho = 0.84$), SO_4^{2-} ($\rho = 0.90$), Na^+ ($\rho = 0.92$), NH_4^+ ($\rho = 0.62$), K^+ ($\rho = 0.84$), Mg^{2+} ($\rho = 0.86$), and Ca^{2+} ($\rho = 0.75$) (Thompson et al., 2018).

Factor 3 explains 2 % of the variance and is loaded in Cd, and to a lesser extent in Bi, Cu, Mn, Ni, Pb, Sn, Tl, and Zn. Although 2 % represents a low variance possibly within the background noise, it could still have a physical significance (Moore and Grinsted, 2009). In order to determine if Factor 3 is physically explainable, its time series scores are plotted with the EFs of Cd, Pb and Zn in Fig. 3.

Factor 3 was found to be significantly ($p < 0.01$) correlated with the EFs of the following 12 metals: Cd ($\rho = 0.92$), Zn ($\rho = 0.92$), Pb ($\rho = 0.80$), and Ni ($\rho = 0.80$) shown in Fig. 2, and Ag ($\rho = 0.62$), Bi ($\rho = 0.60$), Co ($\rho = 0.50$), Cr ($\rho = 0.60$), Cu ($\rho = 0.51$), Mn ($\rho = 0.63$), Sn ($\rho = 0.74$), and Tl ($\rho = 0.64$). This indicates that Factor 3 explains the EFs of the aforementioned metals. A hierarchical cluster analysis using the Ward linkage method and the Euclidan distance measure, and a non-hierarchical (K-means) cluster analysis were performed with Factors 1-3 to explore the possible distribution of TEs into associated groups. (Fig. S5). Both cluster analyses show that Pb and Zn are strongly associated, suggesting these TEs likely have common origins.

3.1 21st Century anthropogenic sources

The Mann–Kendall trend test was used to detect TEs with sustained and significant increasing trends in EF and Excess concentration during the 1971–2015 period. The trend test indicated that Bi, Cd, Ni, Pb, Tl, and Zn, which are loaded in Factor 3, have significant increasing EF and Excess concentration trends. The EFs obtained here using PSAs are much smaller than those calculated using the upper continental crust average (Wedepohl, 1995) and also smaller than those from ice cores with lower dust loads compared to Guliya. Thus, it is necessary to determine which of the TEs mentioned above were significantly more enriched during the 2000–2015 period. For this purpose, two different tests were used, the Mann–Whitney test and the two-sample t-test ($p < 0.0005$). Both tests showed that the EFs and Excess concentrations for the metals, Cd, Zn, Pb, and Ni, are significantly higher during the 2000–2015 period than during the 1971–1990 period. Thus, the following sections will specifically focus on these four TEs and their possible sources.

Back-trajectory frequency distributions were determined to establish the origin of air parcels reaching the Guliya ice cap. Back trajectories (7 days) were calculated daily for the 1992–2015 period for winter (December–January–February) (Fig. 1b) and summer (June–July–August) (Fig. 1c) using the HYSPLIT model from the National Oceanic and Atmospheric Administration. During winter, Guliya is strongly influenced by air parcels mostly from western Xinjiang (China); from Central Asia, which consists of the former Soviet republics of Kazakhstan, Kyrgyzstan, Tajikistan, Turkmenistan, and Uzbekistan; from Afghanistan and Pakistan in South Asia; and to a lesser extent from the Middle East, Northern Africa, and both Eastern and Western Europe. In summer, westerly and southerly (monsoonal) flows, and even occasional northerly flows, influence Guliya, such that the entire Xinjiang region in addition to Central Asia and the northern regions of Afghanistan and Pakistan, lies within the back trajectories area. Air parcels from other Southern Asian countries, such as India and Nepal, can also reach Guliya during summer.

Trace element enrichments in the Guliya core could reflect changes in emissions, atmospheric circulation, and/or post-depositional processes. Post-depositional processes (e.g., seasonal surface melting, percolation and refreezing of meltwater) do not significantly affect the stratigraphy of the Guliya core (Thompson et al., 2018). The Guliya borehole temperatures were between –8°C and –12°C from the surface to ~15 m depth confirming that the ice is cold (Thompson et al., 2018) and that overprinting of the TE records due to meltwater percolation is unlikely to occur. Thus, the enrichments observed in the Guliya record indicate increasing emissions in specific source regions and/or changes in atmospheric circulation.

To determine the origin of the Guliya Cd, Pb, Zn, and Ni enrichments, we examine the most important emission sources of atmospheric TEs from the determined regions of influence: Central Asia, South Asia (Afghanistan, Pakistan, and India), and Xinjiang (China). We also use $PM_{2.5}$ emission estimates, which very likely contain toxic metals such as Cd, Pb, Ni, and Zn, using the EDGAR (Emissions Database for Global Atmospheric Research) v4.3.2 air pollutant dataset (1970–2012) (EDGARv4.3.2, 2017; Crippa et al., 2018). The EDGAR dataset provides total $PM_{2.5}$ and also $PM_{2.5}$ by emission sector for all countries.

In the EDGAR database, the total $PM_{2.5}$ corresponds to emissions from all human activities except large-scale biomass burning and land use, land-use change, and forestry (EDGARv4.3.2, 2017; Crippa et al., 2018). To better understand

the possible emission sources, here we divided the EDGAR $PM_{2.5}$ emission sectors into five source categories in accordance with the 2006 IPCC Guidelines for National Greenhouse Gas Inventories (IPCC, 2006). These source categories include: 1) fossil fuel combustion which comprises the emission sectors: power generation and combustion in the manufacturing, transportation, and residential sectors, 2) biomass burning which includes biofuel combustion in the manufacturing, transportation, and residential emission sectors as well as agricultural waste and field burning, 3) industrial processes which include the emission sectors: mineral, chemical, and metal industry and other production industry (note: this category does not include any type of fossil fuel combustion used by these industries), 4) agriculture which includes the emission sectors: manure management, rice cultivation, direct soil emission, manure in pasture/range/paddock, and other direct soil emissions, and 5) waste which includes the emission sectors: waste incineration and solid waste disposal on land.

In 2012, fossil fuel combustion was the primary source of the total $PM_{2.5}$ emissions in China, Kazakhstan, and Kyrgyzstan (~60–80 %), followed by biomass burning (~20–35 %), industry (~2–10 %), agriculture (~1–3 %), and waste (<1 % for China, no $PM_{2.5}$ emissions estimated for waste incineration for the other countries in the EDGAR database). While biomass burning was the primary $PM_{2.5}$ source in Afghanistan, Pakistan, and Nepal (~80–90 %) and in India, Tajikistan, Uzbekistan, and Turkmenistan (~50–60 %) followed by fossil fuel combustion (~2–15 % and 20–30 %, respectively) and industrial activities (< 2 % and ~2–15 %, respectively) (EDGARv4.3.2, 2017; Crippa et al., 2018). Regarding Xinjiang in particular, numerous studies have estimated coal combustion as a major source of atmospheric Cd, Pb, Zn, and Ni followed by smelting processes as a source of Cd, Pb, and Zn (Li et al., 2012; Shao et al., 2013; Cheng et al., 2014; Tian et al., 2015), and by oil combustion as a source of Ni (Tian et al., 2012) and biomass burning as a source of Cd, Pb, and Ni (Cheng et al., 2014; Tian et al., 2015). Thus, in the following sections we focus on the largest TE and $PM_{2.5}$ source categories: fossil fuel combustion (Sect. 3.1.1), biomass burning (Sect. 3.1.2), metal production (Sect. 3.1.3), and the agricultural sector (Sect. 3.1.4).

3.1.1 Fossil fuel combustion

In the regions that influence Guliya, two distinct trends in fossil fuel consumption emissions are discernible. Firstly, a steady increasing trend since the 1970s is observed in the Xinjiang province, Afghanistan, Pakistan, India, and Nepal (Fig. 4a). Secondly, a decline after the 1990s is observed in Central Asian countries due to the collapse of the Soviet Union (Fig. 4b). India and Xinjiang (China) became the largest consumers of both coal and oil in the region during the 21st century, with coal as their primary energy source (Fig. 4). The third largest consumer of coal and oil in the region during the 21st century is Kazakhstan despite its decreased consumption after the 1990s. Significant positive correlations ($p < 0.001$) were found between the Guliya EFs of Cd, Pb, Zn, and Ni and coal consumption in Xinjiang, India, China, and Pakistan; oil consumption in Xinjiang, India, China, Pakistan, and Turkmenistan; and total $PM_{2.5}$ emissions from China, India, Pakistan and Afghanistan. These positive correlations were expected since these records show generally increasing trends as shown in Fig. 4. Although Pakistan's fossil fuel consumption is 1–2 orders of magnitude lower than that of Xinjiang and India, the Guliya TE enrichments closely resemble Pakistan's coal consumption between 2005 and 2015. Both records peaked in 2008 after which they began to decrease suggesting Pakistan's coal consumption could be one of the sources of anthropogenic TEs observed in the Guliya core.

To further investigate the role of fossil fuel combustion in Pakistan and in the other regions, we examined $PM_{2.5}$ emitted by the different sectors comprising fossil fuel combustion. The most interesting outcome is the temporal correspondence between the Guliya TE enrichments and Pakistan's $PM_{2.5}$ emissions associated with road transportation and manufacturing and construction (M-C) industries, which are the two largest fossil fuel combustion $PM_{2.5}$ emission sectors in Pakistan (Fig. S6). The enrichments of Cd, Pb, Zn, and Ni have two maxima, one in 2000 when $PM_{2.5}$ emissions from road transportation peaked, and the other in 2008 when $PM_{2.5}$ emissions from the M-C industries peaked. After 2008, TE enrichments (except for Pb) and $PM_{2.5}$ emissions (road transportation and M-C industries) decreased (Fig. S6).

Although Pakistan's oil and coal consumption is much lower than that in Xinjiang and India, Pakistan is home to some of the most polluted cities in the world (WHO, 2016) due to the lack of emission controls and air quality standards (Colbeck et al., 2010; Sánchez-Triana et al., 2014). These cities include Peshawar, Rawalpindi, Lahore, Faisalabad, and Pakistan's capital, Islamabad (Rasheed et al., 2014; WHO, 2016; Shi et al., 2018), all located in northern Pakistan from which air parcels have been shown to strongly influence the Guliya site throughout the year. Air parcels from Xinjiang and India, on the other hand, only reach Guliya during summer (Fig. 1c). Thus, fossil fuel combustion emissions from Xinjiang and India but also from Pakistan contribute significantly to the Guliya TE enrichments observed. Nepal's and Afghanistan's fossil fuel consumption have also been increasing and even though it is ~10-100 times lower than those of Xinjiang, India or Pakistan, they are within the high percentage (5-15 %) region of back trajectory frequencies. Thus, fossil fuel emissions from both Nepal and Afghanistan can also reach Guliya. Although fossil fuel consumption has declined in Central Asia since the 1990s, their emissions have also likely contributed to the TE enrichments detected in Guliya since Central Asia is in the high frequency region of the Guliya back trajectories.

3.1.2 Biomass Burning

Total $PM_{2.5}$ emissions from biomass burning have been increasing since 1970 in Pakistan, India and Nepal at a constant rate, and in Afghanistan, Tajikistan, Uzbekistan, and Turkmenistan since ~1995 (Fig. 5). In China, they reached a maximum in 1990 after which they slightly decreased probably due to the increase of fossil fuel consumption. The Guliya TE enrichments do not resemble the biomass burning $PM_{2.5}$ emission trends for any country except for Turkmenistan's that peaks in 2007, one year before the Guliya EF maximum, and then it decreases similarly to the Guliya TE enrichments. The residential sector is the largest contributor of biomass burning $PM_{2.5}$ emissions in China, India, Nepal, and Pakistan followed by agricultural waste burning, conversely, in Central Asia and Afghanistan the burning of agricultural waste is the largest contributor of biomass burning $PM_{2.5}$ followed by the residential sector (EDGARv4.3.2, 2017; Crippa et al., 2018).

Households in developing countries particularly in rural areas of Asia, widely use traditional biomass burning, characterized by its low efficiency and by the lack of emission controls, for heating and cooking (Gumartini, 2009; Chen et al., 2017; Weyant et al., 2019). In 2012, 4513 Gg of $PM_{2.5}$ from biomass burning and 2534 Gg of $PM_{2.5}$ from fossil fuel combustion from all the countries of interest here (except China) were emitted to the atmosphere

(EDGARv4.3.2, 2017; Crippa et al., 2018). Some studies have found higher TE contents in $PM_{2.5}$ emitted from coal combustion than from biomass burning (except for Zn) (Steenari et al., 1999; Ross et al., 2002; Richaud et al., 2004). However, biomass, like fossil fuels, is a complex mixture of organic and inorganic matter and the TEs contents in its $PM_{2.5}$ emissions depend on the type and origin of the biomass and on its burning conditions (Christian et al., 2010; Vassilev et al., 2013). Thus, while $PM_{2.5}$ from biomass burning is almost twice that from fossil fuel combustion, we can only conclude that biomass burning emissions from Central Asia, South Asia and Xinjiang likely have significantly contributed, like fossil fuels, to the TEs enrichments detected in the Guliya ice cap.

Large-scale biomass burning events, excluded in the EDGAR database, can be another source of atmospheric TEs. In the regions of interest here, fire activity and its emissions decreased in Central Asia and in northwest China between 1997 and 2016. However they increased in India (including northwestern India) and in Nepal, both of which are in the high percentage back trajectory frequency of Guliya (Fig. S7) (van der Werf et al., 2017; You et al., 2018). Thus, emissions from the increased fire activity in India and Nepal probably contribute to the enrichments observed in the Guliya ice core.

3.1.3 Metal production

Like fossil fuel consumption, metal production has increased in Asia since the 1980s (Fig. S8) being China, India and Kazakhstan the most important non-ferrous metal producers in the region and in the world (BGS, 2015). In China, most of the non-ferrous metal production is located in the coastal regions while all Ni production is located in the western region of China (Gansu, Xinjiang, Chongqing, Yunnan, and Liaoning provinces). Gansu, just east of Xinjiang, produces 95 % of the total Ni production in China (Yanjia and Chandler, 2010). The Guliya TE enrichment trends do not resemble those of metal production in China, Pakistan, India nor Kazakhstan (Fig. S8). Thus, although these important metal production sources are relatively close to Guliya, they are likely not the primary source of the Guliya TE enrichments.

$PM_{2.5}$ emissions by industrial processes contribute 10 % of the total $PM_{2.5}$ emissions in China, and 2 % to the total $PM_{2.5}$ emissions in India, Pakistan, and Kazakhstan. Pakistan's $PM_{2.5}$ emissions by industrial processes peaked in 2008 similarly to the Guliya TE enrichments, but they remained relatively stable after 2008 while the Guliya TE enrichments decreased (Fig. S8). Thus, while the increasing emissions from metal production could also influence the TE depositions observed in Guliya, the metal production temporal trends and the industrial $PM_{2.5}$ emissions suggest they are not the main sources of the Guliya TE enrichments.

3.1.4 Agricultural activities

Emissions from agricultural activities are an important source of atmospheric $PM_{2.5}$ worldwide (Lelieveld et al., 2015; Bauer et al., 2016). Fertilizers and pesticides can be a direct (aerial spreading) or indirect (soil exposed to wind erosion) source of toxic metals such as As, Cd, Cu, Cr, Pb, Ni, Zn, and others to the atmosphere (Nriagu and Pacyna, 1988; Nriagu, 1989b). In particular, fertilizers derived from phosphate rocks contain heavy metal impurities such as Cd and Pb that can contaminate agricultural soils (Mortvedt, 1995; Roberts, 2014). While consumption of phosphate fertilizers

decreased in Central Asia in the 1990s, it has been increasing in China, Pakistan, India, and Nepal since the 1970s (Fig. S9). The Guliya TE enrichments resemble neither the phosphate fertilizer consumption records in these countries nor their $PM_{2.5}$ emissions from agricultural activities (Fig. S9). However, emissions associated with agricultural activities in western China, Pakistan, India, and Nepal are likely becoming more important sources of atmospheric TEs since they have been increasing recently and they originate in the back trajectory high frequency regions for Guliya.

Although practically all human activities that emit $PM_{2.5}$ and toxic metals have been increasing in South Asia and in Northwest China, it is very likely that emissions from fossil fuel combustion and biomass burning have dominated the Guliya Cd, Pb, Zn, and Ni enrichments during the 21st century. Emissions from other sources such as industrial processes, agriculture activities, waste disposal, and land-use change have also likely been deposited on the Guliya ice cap. Although economic activities in Central Asia have declined since the 1990s, emissions from their different sectors also probably contribute to the TE enrichments observed in Guliya during the 21st century.

China is investing heavily in global infrastructure projects like the Belt and Road Initiative (New Silk Road), the Western Development policy, and the Pakistan-China Economic Corridor (PCEP) that could potentially increase the emission of atmospheric toxic TEs. These projects were established to improve the economic connectivity with the West and with other countries in the region by modernizing and building new airports, railways, highways, water infrastructure, and power lines. In Pakistan energy was generated mostly from oil, gas, and hydropower until 2015. After the establishment of the PCEP, five coal-fired power plants were built and have been operational since 2017. Three additional plants are expected to open in 2019 and more are currently under construction (CPEC, 2019). These developing projects and the shift to coal-generated power could have severe environmental and human health impacts in the region if mitigation actions are not taken.

4 Conclusions

A new continuous, high-resolution ice core record of trace elements covering the 1971–2015 period was extracted from the Guliya ice cap in Northwestern Tibet, China. This new record extends our previous 1650–1991 Guliya record well into the 21st century making it, the first and most up to date ice core-derived archive of trace metal contamination in the Third Pole region. Since the dust concentrations in the Guliya ice cores are extremely high in comparison to other ice cores from the Third Pole as shown in Sierra-Hernandez et al. (2018), we also used EF and Excess concentrations to differentiate between crustal and non-crustal origins in this new record. Increases in EF and Excess concentrations of Cd, Pb, Zn, and Ni are observed since the 1990s, reaching a maximum in 2008. The enrichments of Cd, Pb, Zn, and Ni increased by ~75 %, 35 %, 30 %, and 10 %, respectively, during the 2000–2015 period relative to 1971–1990. Comparisons between the Cd, Pb, Zn, and Ni enrichments from the Guliya records and fossil fuel consumption, metal production, phosphate fertilizer consumption, and $PM_{2.5}$ emissions from Xinjiang (China), Afghanistan, Pakistan, India, Nepal, and Central Asia suggest that the metal enrichments detected in Guliya originate primarily from fossil fuel combustion and biomass burning in these regions and secondarily from industrial processes and agricultural activities. This new Guliya ice core record demonstrates that the current emissions in Asia are

impacting remote high-altitude glaciers in the region. Therefore, mitigation policies and technologies should be enforced by the governments of Central and South Asian countries to improve the air quality in the region as most Asian countries continue to develop.

Data availability.

Supplement. The Supplement is available online

Author contributions. R.S.H. wrote the paper, performed all the data analysis, interpreted the data, and ran the daily HYSPLIT back trajectories; R.S.H. and E.B. prepared the ice core samples and conducted their ICP-MS analysis; E.B. created the maps for Fig. 1. All authors contributed to the study design, data interpretation, revision and edition of the manuscript. P.G. oversees the ICP-MS lab. L.G.T. planned the drilling operation and led the field expedition in which both L.G.T. and P.G. contributed to the ice core processing in the field.

Competing interests. The authors declare no competing financial interests.

Acknowledgments

The NSF P2C2 program (1502919) funded this study. We thank everybody that made the 2015 Guliya field expedition a success, in particular Tandong Yao from the Institute for Tibetan Plateau Research. The authors greatly acknowledge Julien Nicolas for creating the seasonal back trajectory frequencies grid for all our Guliya TEs publications as well as for his time discussing them. We thank Aaron Wilson for his insights on the meteorology of the region. We thank Xiaoxing Yang and Chao You for providing recent energy yearbook data from Xinjiang. We also thank Max Woodworth for helpful discussions about development projects and policies in western China. We are grateful to Ellen Mosley-Thompson and Mary Davis for valuable comments throughout the development of the manuscript. Stacy Porter is greatly acknowledged for her help in editing and improving the English of the different versions of the manuscript. Lastly, we thank Henry Brecher for his detailed proofreading of the manuscript.

References

Alves, C. A., Gonçalves, C., Pio, C. A., Mirante, F., Caseiro, A., Tarelho, L., Freitas, M. C., and Viegas, D. X.: Smoke emissions from biomass burning in a Mediterranean shrubland, Atmos. Environ., 44, 3024-3033, https://doi.org/10.1016/j.atmosenv.2010.05.010, 2010.

Bauer, S. E., Tsigaridis, K., and Miller, R.: Significant atmospheric aerosol pollution caused by world food cultivation, Geophys. Res. Let., 43, 5394-5400, 10.1002/2016gl068354, 2016.

Beaudon, E., Gabrielli, P., Sierra-Hernández, M. R., Wegner, A., and Thompson, L. G.: Central Tibetan Plateau atmospheric trace metals contamination: A 500-year record from the Puruogangri ice core, Sci. Total Environ., 601-602, 1349-1363, 2017.

BGS, British Geological Survey. World Mineral Statistics and World Mineral Production, 2/1/2018, 2015.

BP, British Petroleoum (BP) Statistical Review of World Energy, 6/20/2016, 9/20/2016, 2016.

Chen, J., Li, C., Ristovski, Z., Milic, A., Gu, Y., Islam, M. S., Wang, S., Hao, J., Zhang, H., He, C., Guo, H., Fu, H., Miljevic, B., Morawska, L., Thai, P., Lam, Y. F., Pereira, G., Ding, A., Huang, X., and Dumka, U. C.: A review of biomass burning: Emissions and impacts on air quality, health and climate in China, Sci. Total Environ., 579, 1000-1034, https://doi.org/10.1016/j.scitotenv.2016.11.025, 2017.

Chen, P., Kang, S., Bai, J., Sillanpää, M., and Li, C.: Yak dung combustion aerosols in the Tibetan Plateau: Chemical characteristics and influence on the local atmospheric environment, Atmos. Res., 156, 58-66, https://doi.org/10.1016/j.atmosres.2015.01.001, 2015.

Chen, W., Li, H., and Wu, Z.: Western China energy development and west to east energy transfer: Application of the Western China Sustainable Energy Development Model, Energy Policy, 38, 7106-7120, 2010.

Cheng, K., Tian, H. Z., Zhao, D., Lu, L., Wang, Y., Chen, J., Liu, X. G., Jia, W. X., and Huang, Z.: Atmospheric emission inventory of cadmium from anthropogenic sources, Int. J. Environ. Sci. Technol., 11, 605-616, 10.1007/s13762-013-0206-3, 2014.

Christian, T. J., Yokelson, R. J., Cárdenas, B., Molina, L. T., Engling, G., and Hsu, S. C.: Trace gas and particle emissions from domestic and industrial biofuel use and garbage burning in central Mexico, Atmos. Chem. Phys., 10, 565-584, 10.5194/acp-10-565-2010, 2010.

Colbeck, I., Nasir, Z. A., and Ali, Z.: The state of ambient air quality in Pakistan—a review, Environ. Sci. Pollut. R., 17, 49-63, 10.1007/s11356-009-0217-2, 2010.

Cooke, C. A., and Bindler, R.: Lake Sediment Records of Preindustrial Metal Pollution, in: Environmental Contaminants. Developments in Paleoenvironmental Research, edited by: Blais, J., Rosen, M., and Smol, J., Springer, Dordrecht, 101-119, 2015.

China Pakistan Economic Corridor: http://cpec.gov.pk/, access: 4 April 2019, 2019.

Crippa, M., Guizzardi, D., Muntean, M., Schaaf, E., Dentener, F., van Aardenne, J. A., Monni, S., Doering, U., Olivier, J. G. J., Pagliari, V., and Janssens-Maenhout, G.: Gridded emissions of air pollutants for the period 1970–2012 within EDGAR v4.3.2, Earth Syst. Sci. Data, 10, 1987-2013, 10.5194/essd-10-1987-2018, 2018.

Dong, W., and Yang, Y.: Exploitation of mineral resource and its influence on regional development and urban evolution in Xinjiang, China, J. Geog. Sc., 24, 1131-1146, 10.1007/s11442-014-1143-x, 2014.

EDGARv4.3.2, European Commission, Joint Research Centre (EC-JRC)/Netherlands Environmental Assessment Agency (PBL). Emissions Database for Global Atmospheric Research (EDGAR), release EDGAR v4.3.2 (1970 - 2012), 2017.

EIA, U.S. Energy Information Administration, 2/28/2019, 2019.

Fridley, D., Lu, H., and Liu, X.: China Energy Databook 9.0, 9th ed., edited by: Group, C. E., Lawrence Berkeley National Laboratory, United States, 2017.

Gabrielli, P., and Vallelonga, P.: Contaminant Records in Ice Cores, in: Environmental Contaminants. Developments in Paleoenvironmental Research, edited by: Blais, J., Rosen, M., and Smol, J., Springer, Dordrecht, 393-430, 2015.

Gumartini, T.: Biomass energy in the Asia-pacific region: current status, trends and future setting, FAO Regional Office, Bangkok, 2009.

Hansson, S., Bindler, R., and De Vleeschouwer, F.: Using Peat Records as Natural Archives of Past Atmospheric Metal Deposition, in: Environmental Contaminants. Developments in Paleoenvironmental Research, edited by: Blais, J., Rosen, M., and Smol, J., Springer, Dordrecht, 323-354, 2015.

IPCC: 2006 IPCC Guidelines for National Greenhouse Gas Inventories, in, edited by: Eggleston, S., Buendia, L., Miwa, K., Ngara, T., and Tanabe, K., Hayama, Japan, 2006.

Lai, H. H.: China's Western Development Program: Its Rationale, Implementation, and Prospects, Modern China, 28, 432-466, 2002.

Lelieveld, J., Evans, J. S., Fnais, M., Giannadaki, D., and Pozzer, A.: The contribution of outdoor air pollution sources to premature mortality on a global scale, Nature, 525, 367-371, 10.1038/nature15371, 2015.

Li, Q., Cheng, H., Zhou, T., Lin, C., and Guo, S.: The estimated atmospheric lead emissions in China, 1990-2009, Atmos. Environ., 60, 1-8, 2012.

Liu, F., Zhang, Q., Tong, D., Zheng, B., Li, M., Huo, H., and He, K. B.: High-resolution inventory of technologies, activities, and emissions of coal-fired power plants in China from 1990 to 2010, Atmos. Chem. Phys., 15, 13299-13317, 10.5194/acp-15-13299-2015, 2015.

Marx, S. K., and McGowan, H. A.: Long-Distance Transport of Urban and Industrial Metals and Their Incorporation into the Environment: Sources, Transport Pathways and Historical Trends, in: Urban Airborne Particulate Matter. Origin, Chemistry, Fate and Health Impacts, edited by: Zereini, F., and Wiseman, C. L. S., Springer, Berlin, 103-123, 2010.

Marx, S. K., Rashid, S., and Stromsoe, N.: Global-scale patterns in anthropogenic Pb contamination reconstructed from natural archives, Environ. Pollut., 213, 283-298, 2016.

Moore, J. C., and Grinsted, A.: Ion Fractionation and Percolation in Ice Cores with Seasonal Melting, Physics of Ice Core Records II, Suppl Issue of Low Temperature Science, 68, 287-298, 2009.

Mortvedt, J. J.: Heavy metal contaminants in inorganic and organic fertilizers, Fertilizer Res., 43, 55-61, 10.1007/bf00747683, 1995.

Ning, J.: China Statistical Yearbook, 2016.

Nriagu, J. O., and Pacyna, J. M.: Quantitative assessment of worldwide contamination of air, water and soils by trace metals, Nature, 333, 134-139, 1988.

Nriagu, J. O.: Natural Versus Anthropogenic Emissions of Trace Metals to the Atmosphere, in: Control and Fate of Atmospheric Trace Metals, edited by: Pacyna, J., and Ottar, B., Mathematical and Physical Sciences, 268, Kluwer Academic Publishers, 3-13, 1989a.

Nriagu, J. O.: A global assessment of natural sources of atmospheric trace metals, Lett. Nature, 338, 47-49, 1989b.

Pacyna, J. M., and Pacyna, E. G.: An assessment of global and regional emissions of trace metals to the atmosphere from anthropogenic sources worldwide, Environ. Rev., 9, 269-298, 2001.

Rasheed, A., Aneja, V. P., Aiyyer, A., and Rafique, U.: Measurements and analysis of air quality in Islamabad, Pakistan, Earth's Future, 2, 303-314, 10.1002/2013ef000174, 2014.

Reddy, M. S., Basha, S., Joshi, H. V., and Jha, B.: Evaluation of the emission characteristics of trace metals from coal and fuel oil fired power plants and their fate during combustion, J. Hazard. Mater., 123, 242-249, http://dx.doi.org/10.1016/j.jhazmat.2005.04.008, 2005.

Richaud, R., Herod, A. A., and Kandiyoti, R.: Comparison of trace element contents in low-temperature and high-temperature ash from coals and biomass, Fuel, 83, 2001-2012, https://doi.org/10.1016/j.fuel.2004.05.009, 2004.

Roberts, T. L.: Cadmium and Phosphorous Fertilizers: The Issues and the Science, Procedia Eng., 83, 52-59, https://doi.org/10.1016/j.proeng.2014.09.012, 2014.

Rolph, G., Stein, A., and Stunder, B.: Real-time Environmental Applications and Display sYstem: READY, Environ. Model. Softw., 95, 210-228, 2017.

Ross, A. B., Jones, J. M., Chaiklangmuang, S., Pourkashanian, M., Williams, A., Kubica, K., Andersson, J. T., Kerst, M., Danihelka, P., and Bartle, K. D.: Measurement and prediction of the emission of pollutants from the combustion of coal and biomass in a fixed bed furnace, Fuel, 81, 571-582, https://doi.org/10.1016/S0016-2361(01)00157-0, 2002.

Sánchez-Triana, E., Enriquez, S., Afzal, J., and Nakawaga, A.: Air Pollution in Pakistan, in: Cleaning Pakistan's Air: Policy Options to Address the Cost of Outdoor Air Pollution, 57-81, 2014.

Shao, X., Cheng, H., Li, Q., and Lin, C.: Anthropogenic atmospheric emissions of cadmium in China, Atmos. Environ., 79, 155-160, 2013.

Shi, Y., Matsunaga, T., Yamaguchi, Y., Li, Z., Gu, X., and Chen, X.: Long-term trends and spatial patterns of satellite-retrieved $PM_{2.5}$ concentrations in South and Southeast Asia from 1999 to 2014, Sci. Total Environ., 615, 177-186, https://doi.org/10.1016/j.scitotenv.2017.09.241, 2018.

Sierra-Hernández, M. R., Gabrielli, P., Beaudon, E., Wegner, A., and Thompson, L. G.: Atmospheric depositions of natural and anthropogenic trace elements on the Guliya ice cap (northwestern Tibetan Plateau) during the last 340 years, Atmos. Environ., 176, 91-102, 2018.

Singh, N., Banerjee, T., Raju, M. P., Deboudt, K., Sorek-Hamer, M., Singh, R. S., and Mall, R. K.: Aerosol chemistry, transport, and climatic implications during extreme biomass burning emissions over the Indo-Gangetic Plain, Atmos. Chem. Phys., 18, 14197-14215, 10.5194/acp-18-14197-2018, 2018.

Steenari, B. M., Schelander, S., and Lindqvist, O.: Chemical and leaching characteristics of ash from combustion of coal, peat and wood in a 12MW CFB – a comparative study, Fuel, 78, 249-258, https://doi.org/10.1016/S0016-2361(98)00137-9, 1999.

Stein, A. F., Draxler, R. R., Rolph, G. D., Stunder, B. J. B., Cohen, M. D., and Ngan, F.: NOAA's HYSPLIT Atmospheric Transport and Dispersion Modeling System, Bull. Am. Meteorol. Soc., 96, 2059-2077, 10.1175/bams-d-14-00110.1, 2015.

Thompson, L. G., Mosley-Thompson, E., Davis, M. E., Lin, P.-N., Mikhalenko, V., and Dai, J.: A 1000 year ice core climate record from the Guliya Ice Cap, China and its relationship to global climate variability, Ann. Glaciol., 21, 175-181, 1995.

514 Thompson, L. G., Yao, T., Davis, M. E., Mosley-Thompson, E., Wu, G., Porter, S. E., Xu, B., Lin, P.-N., Wang, N.,
515 Beaudon, E., Duan, K., Sierra-Hernández, M. R., and Kenny, D. V.: Ice core records of climate variability on the
516 Third Pole with emphasis on the Guliya ice cap, western Kunlun Mountains, Quat. Sci. Rev., 188, 1-14, 2018.
517 Tian, H. Z., Lu, L., Cheng, K., Hao, J. M., Zhao, D., Wang, Y., Jia, W. X., and Qiu, P. P.: Anthropogenic
518 atmospheric nickel emissions and its distribution characteristics in China, Sci. Total Environ., 417-418, 148-157,
519 https://doi.org/10.1016/j.scitotenv.2011.11.069, 2012.
520 Tian, H. Z., Zhu, C. Y., Gao, J. J., Cheng, K., Hao, J. M., Wang, K., Hua, S. B., Wang, Y., and Zhou, J. R.:
521 Quantitative assessment of atmospheric emissions of toxic heavy metals from anthropogenic sources in China:
522 historical trend, spatial distribution, uncertainties, and control policies, Atmos. Chem. Phys., 15, 10127-10147,
523 2015.
524 Uglietti, C., Gabrielli, P., Olesik, J. W., Lutton, A., and Thompson, L. G.: Large variability of trace element mass
525 fractions determined by ICP-SFMS in ice core samples from worldwide high altitude glaciers, Appl. Geochem., 47,
526 109-121, 2014.
527 UN, United Nations. Department of Economic and Social Affairs, Population Division. World Population Prospects:
528 The 2017 Revision, 2017.
529 van der Werf, G. R., Randerson, J. T., Giglio, L., van Leeuwen, T. T., Chen, Y., Rogers, B. M., Mu, M., van Marle,
530 M. J. E., Morton, D. C., Collatz, G. J., Yokelson, R. J., and Kasibhatla, P. S.: Global fire emissions estimates during
531 1997–2016, Earth Syst. Sci. Data, 9, 697-720, 10.5194/essd-9-697-2017, 2017.
532 Vassilev, S. V., Baxter, D., Andersen, L. K., and Vassileva, C. G.: An overview of the composition and application
533 of biomass ash. Part 1. Phase–mineral and chemical composition and classification, Fuel, 105, 40-76,
534 https://doi.org/10.1016/j.fuel.2012.09.041, 2013.
535 Wedepohl, K. H.: The composition of the continental crust, Geochim. Cosmochim. Acta, 59, 1217-1232, 1995.
536 Weyant, C. L., Chen, P., Vaidya, A., Li, C., Zhang, Q., Thompson, R., Ellis, J., Chen, Y., Kang, S., Shrestha, G. R.,
537 Yagnaraman, M., Arineitwe, J., Edwards, R., and Bond, T. C.: Emission Measurements from Traditional Biomass
538 Cookstoves in South Asia and Tibet, Environ. Sci. Technol., 53, 3306-3314, 10.1021/acs.est.8b05199, 2019.
539 WHO, World Health Organization. Ambient Air Pollution Database, 2016.
540 Xu, M., Yan, R., Zheng, C., Qiao, Y., Han, J., and Sheng, C.: Status of trace element emission in a coal combustion
541 process: a review, Fuel Process. Technol., 85, 215-237, http://dx.doi.org/10.1016/S0378-3820(03)00174-7, 2004.
542 Yanjia, W., and Chandler, W.: The Chinese nonferrous metals industry—energy use and CO_2 emissions, Energy
543 Policy, 38, 6475-6484, 10.1016/j.enpol.2009.03.054, 2010.
544 You, C., Yao, T., and Xu, C.: Recent Increases in Wildfires in the Himalayas and Surrounding Regions Detected in
545 Central Tibetan Ice Core Records, J. Geophys. Res.: Atmospheres, 123, 3285-3291, 10.1002/2017jd027929, 2018.
546 Zhang, W., Tong, Y., Wang, H., Chen, L., Ou, L., Wang, X., Liu, G., and Zhu, Y.: Emission of metals from
547 pelletized and uncompressed biomass fuels combustion in rural household stoves in China, Sci. Rep., 4, 5611-5611,
548 10.1038/srep05611, 2014.

549

550

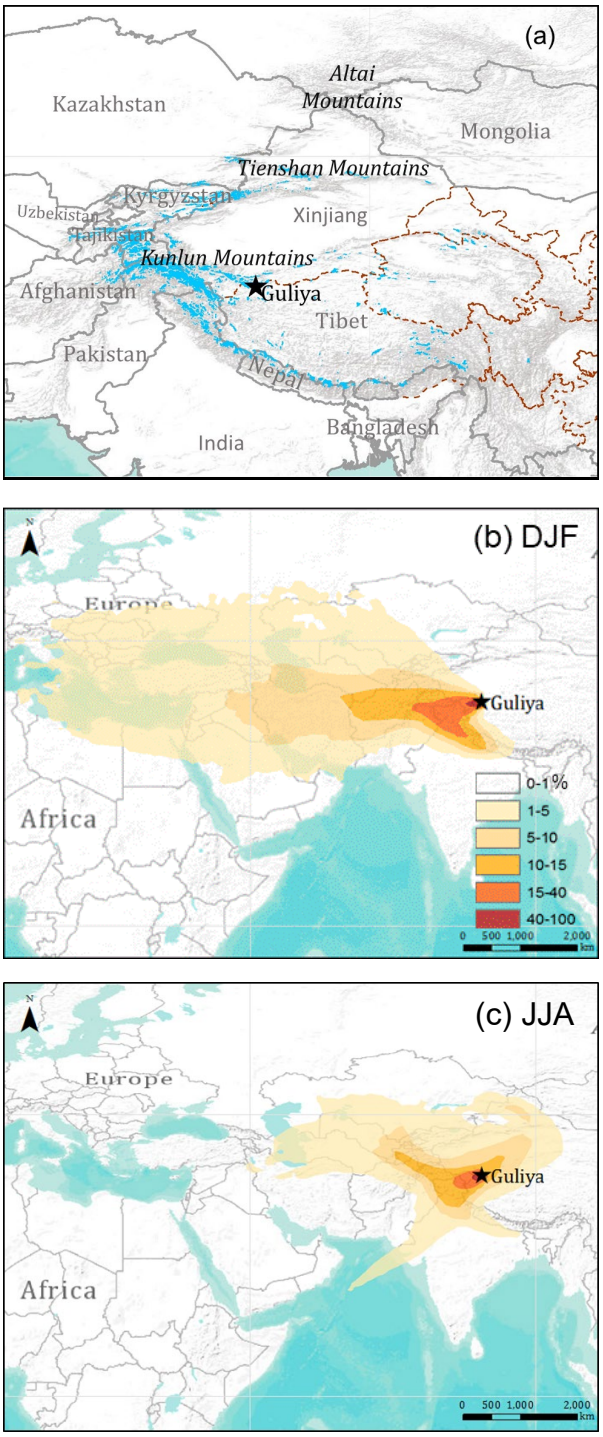

Figure 1. Maps showing the location of the Guliya ice cap (star) and the three mountain ranges of the Xinjiang province (a), and seasonal NOAA HYSPLIT 7-day back trajectories frequency plots for December, January, and February (b); and June, July, and August (c) for the 1992–2015 period (Rolph et al., 2017; Stein et al., 2015).

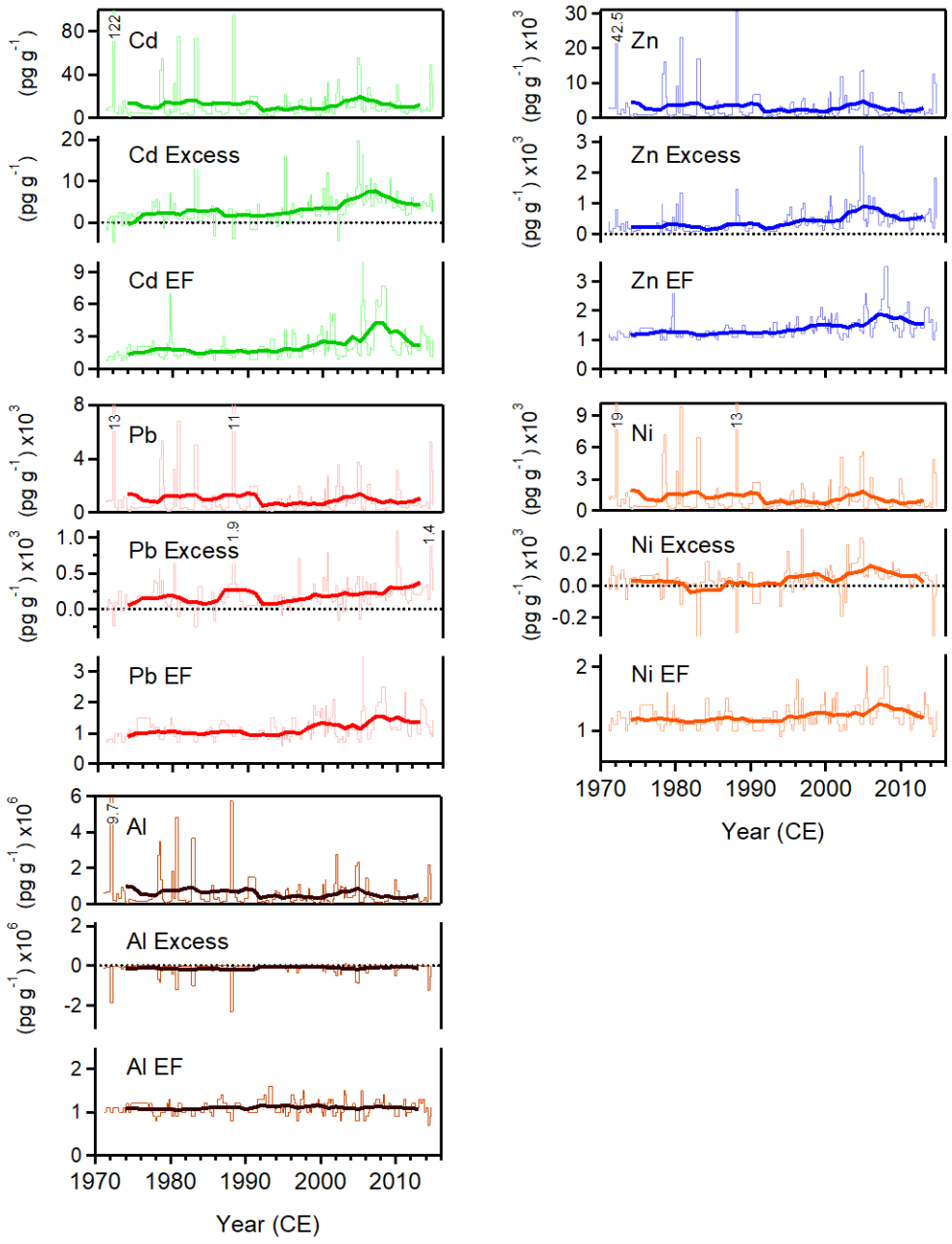

557

558 **Figure 2**. Cd, Pb, Zn, Ni, and Al 5-year running means (thick lines) of concentrations, Excess concentrations, and
559 EFs between 1971 and 2015. Thin lines show the sample resolution.

560

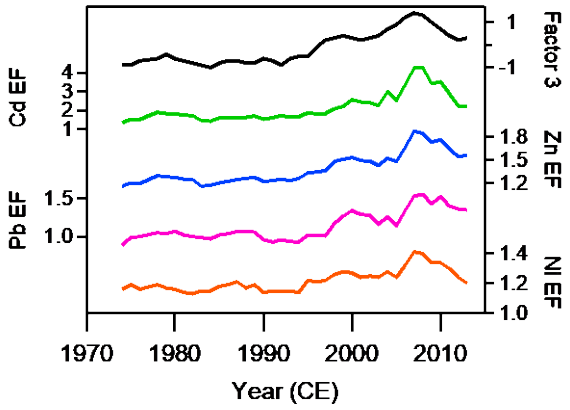

561

562 **Figure 3.** Comparison of 5-year running means of Factor 3 scores with Cd, Zn, Pb, and Ni EFs between 1971 and
563 2015.

564

565

566

567

568

569

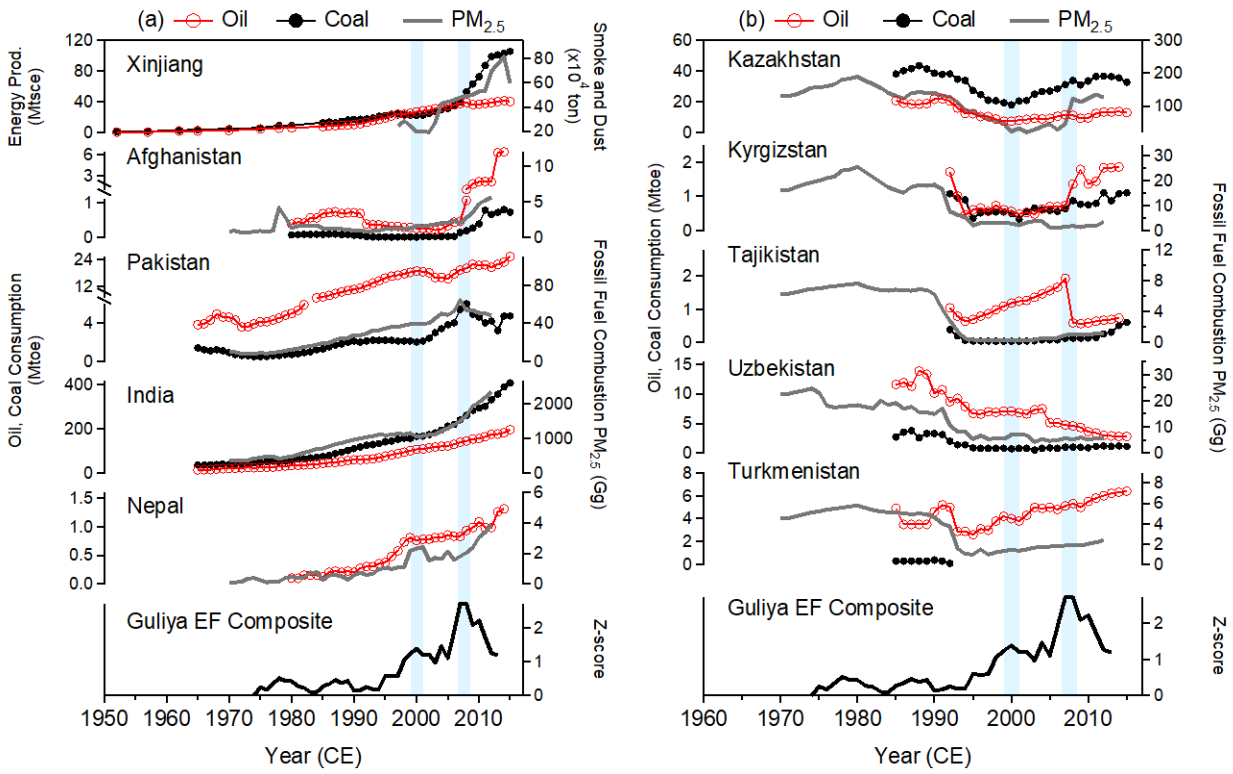

570

571 **Figure 4.** Oil and coal consumption in: (a) Xinjiang, as coal energy production in million tonnes of standard coal
572 equivalent (Jianxin, 2016); in million tonnes of oil equivalent (Mtoe) in Afghanistan (EIA, 2019), Pakistan (BP,
573 2016), India (BP, 2016), and Nepal (coal ≤ 0.1 Mtoe) (EIA, 2019). (b) Central Asian countries: Kazakhstan (BP,
574 2016), Kyrgizstan and Tajikistan (EIA, 2019), and Uzbekistan and Turkmenistan (BP, 2016). $PM_{2.5}$ emissions from
575 fossil fuel combustion sources (EDGARv4.3.2, 2017; Crippa et al., 2018) shown in both panels for all countries
576 except Xinjiang (China). Smoke and dust emissions from Xinjiang (Ning, 2016) are shown since no $PM_{2.5}$ data was
577 available. The Guliya EF composite (average of Cd, Pb, Zn, and Ni EF z-scores) is shown at the bottom of each
578 panel for comparison. The two Guliya maxima at 2000 and 2008 are shown as shaded bars.

579

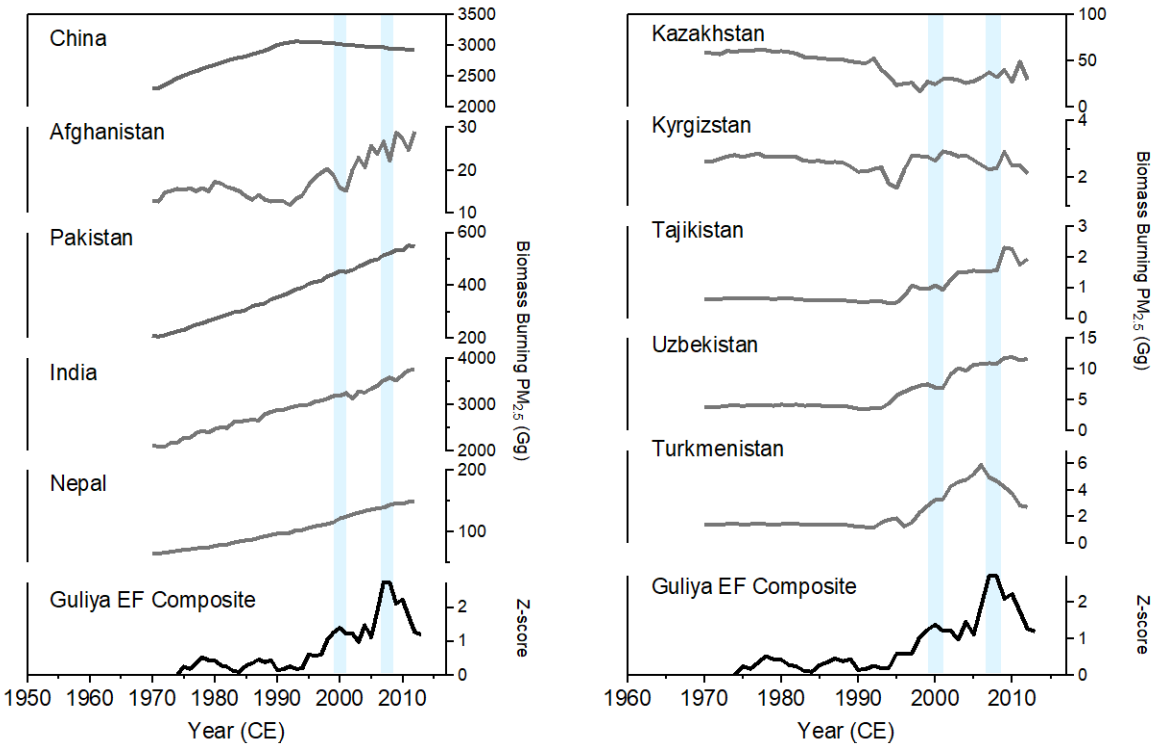

580

581 **Figure 5.** $PM_{2.5}$ emissions from biomass burning sources (EDGARv4.3.2, 2017; Crippa et al., 2018) shown in both
582 panels for all countries. The Guliya EF composite (average of Cd, Pb, Zn, and Ni EF z-scores) is shown at the
583 bottom of each panel for comparison. The two Guliya maxima at 2000 and 2008 are shown as shaded bars.